









OCTOBER 02 2023

Implications of porpoise echolocation and dive behaviour on passive acoustic monitoring

Jamie Donald John Macaulay ; Laia Rojano-Doñate ; Michael Ladegaard ; Jakob Tougaard ; Jonas Teilmann ; Tiago A. Marques ; Ursula Siebert ; Peter Teglberg Madsen 



J. Acoust. Soc. Am. 154, 1982–1995 (2023)

<https://doi.org/10.1121/10.0021163>



View
Online



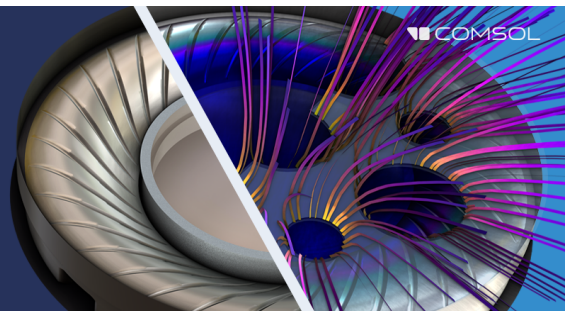
Export
Citation

CrossMark









Take the Lead in Acoustics

The ability to account for coupled physics phenomena lets you predict, optimize, and virtually test a design under real-world conditions – even before a first prototype is built.

» Learn more about COMSOL Multiphysics®



Implications of porpoise echolocation and dive behaviour on passive acoustic monitoring

Jamie Donald John Macaulay,^{1,a)}  Laia Rojano-Doñate,¹  Michael Ladegaard,¹  Jakob Tougaard,² 
Jonas Teilmann,²  Tiago A. Marques,^{3,b)}  Ursula Siebert,^{2,c)}  and Peter Teglberg Madsen¹ 

¹Department of Biology–Zoophysiology, Aarhus University, C. F. Møllers Allé 3, building 1131, 8000 Aarhus C, Denmark

²Department of Ecoscience–Marine Mammal Research, Aarhus University, Frederiksborgvej 399, 4000 Roskilde, Denmark

³Centre for Research into Ecological and Environmental Modelling, University of St. Andrews, St. Andrews, Scotland, United Kingdom

ABSTRACT:

Harbour porpoises are visually inconspicuous but highly soniferous echolocating marine predators that are regularly studied using passive acoustic monitoring (PAM). PAM can provide quality data on animal abundance, human impact, habitat use, and behaviour. The probability of detecting porpoise clicks within a given area (\hat{P}) is a key metric when interpreting PAM data. Estimates of \hat{P} can be used to determine the number of clicks per porpoise encounter that may have been missed on a PAM device, which, in turn, allows for the calculation of abundance and ideally non-biased comparison of acoustic data between habitats and time periods. However, \hat{P} is influenced by several factors, including the behaviour of the vocalising animal. Here, the common implicit assumption that changes in animal behaviour have a negligible effect on \hat{P} between different monitoring stations or across time is tested. Using a simulation-based approach informed by acoustic biologging data from 22 tagged harbour porpoises, it is demonstrated that porpoise behavioural states can have significant (up to 3× difference) effects on \hat{P} . Consequently, the behavioural state of the animals must be considered in analysis of animal abundance to avoid substantial over- or underestimation of the true abundance, habitat use, or effects of human disturbance.

© 2023 Author(s). All article content, except where otherwise noted, is licensed under a Creative Commons Attribution (CC BY) license (<http://creativecommons.org/licenses/by/4.0/>). <https://doi.org/10.1121/10.0021163>

(Received 28 March 2023; revised 31 August 2023; accepted 6 September 2023; published online 2 October 2023)

[Editor: Brian Branstetter]]

Pages: 1982–1995

I. INTRODUCTION

Studies of porpoises and other odontocetes using passive acoustic monitoring (PAM) rely on the assumption of a stable or known relationship between the vocalisations of animals and detections on a PAM device. Under this assumption, changes in detection rates can be used as a robust indicator of changes in the density of porpoises and allow for comparing acoustic data in space (between different recording stations) and time (for example, circatidal, circadian and seasonal rhythm, or levels of disturbance). However, acoustic data collected on PAM devices are affected by a complex mix of factors relating to the environment and behaviour of clicking porpoises. For example, the narrow sound beam (Koblitz *et al.*, 2012; Macaulay *et al.*, 2020), variable source levels (SLs; Villadsgaard *et al.*, 2007), and sound production rates of porpoises (Wisniewska *et al.*, 2016) along with changes in diving behaviour may have a significant influence on the likelihood that porpoise

clicks are detected. As these factors can change across different habitats and times, PAM studies must consider the *probability of detecting* target sounds at different recording sites and over time to allow for a comparison across recorders. This probability of detection, which usually expresses the likelihood that a porpoise or individual click is detected, provides an estimate of the number of porpoise/clicks (and, hence, ultimately animals) likely to have been missed within the monitored area. If estimated correctly, a correction for detection probability allows for the unbiased comparison of acoustic data across different habitats, times, and environmental conditions. Furthermore, if unbiased estimates of click rates can be obtained, the detection rates may be used to calculate absolute animal abundance (e.g., Marques *et al.*, 2009; Warren *et al.*, 2017; Amundin *et al.*, 2022).

There are several ways to determine probability of detection. Any PAM system which can calculate distances to detected animals (static or towed array systems; for example, Barlow and Taylor, 2005) can use the decreasing number of detections with range to estimate detection probabilities *in situ*. If range cannot be calculated, then detection probabilities can be estimated by combining acoustic data and prior knowledge on animal behaviour (e.g., dive depth distribution; Barlow *et al.*, 2021) or tagging animals with acoustic loggers within a study area (Marques *et al.*, 2009). When neither direct range nor using prior behavioural information is possible (usually when using

^{a)}Also at: Sea Mammal Research Unit, Scottish Oceans Institute, Institiud Chuantan na h-Alba, University of St. Andrews, Gatty Marine Laboratory, East Sands, St. Andrews, KY16 8LB, Scotland, UK. Email: jdjm@st-andrews.ac.uk

^{b)}Also at: Departamento de Biologia Animal, Centro de Estatística e Aplicações, Faculdade de Ciências da Universidade de Lisboa.

^{c)}Also at: Institute for Terrestrial and Aquatic Wildlife Research, University of Veterinary Medicine Hannover, 25761 Buesum, Germany.

single channel static devices), separate external experiments can be performed to calculate the probability of detection; however, such experiments are often complex and time consuming (e.g., [Kyhn et al., 2012](#); [Nuutila et al., 2013](#); [Nuutila et al., 2018](#)). Using static single channel recording devices deployed in areas with little prior or no knowledge on animal behaviour to estimate detection probabilities is, therefore, a particularly difficult case. For many of these static PAM surveys, detection probabilities, if estimated at all, are usually calculated for a small subset of devices, and then extrapolated to other devices and time periods (e.g., [Amundin et al., 2022](#)). In such cases, or for any study that ignores detection probability, it is assumed either deliberately for pragmatic reasons or implicitly that environmental and/or behavioural effects at different sites are random with respect to the factors under investigation and, therefore, average out. Understanding whether this assumption is valid is key to understanding the efficacy of current PAM methods and informing future monitoring strategies. Of particular importance is the question as to what degree the behaviour of porpoises affects the detection probability, as such a dependency would introduce behaviour as a confounding factor when assessing observed differences in detection rates over time or between stations. This problem is particularly relevant if, for example, anthropogenic noise, different habitats, and/or seasonal changes alter the behaviour of the clicking porpoises.

Harbour porpoises are known to employ different foraging strategies in time and space ([Wisniewska et al., 2016](#); [Wisniewska et al., 2018b](#); [Rojano-Doñate, 2020](#)), targeting pelagic and benthic fish species ([Börjesson et al., 2003](#); [Jansen et al., 2013](#); [Andreasen et al., 2017](#)). They have also been shown to use eddies to exploit narrow tidal races ([Pierpoint, 2008](#)) and hunt collaboratively on schools of fish ([Torres Ortiz et al., 2021](#)). Consequently, it is reasonable to assume that such a wide range of behaviours may introduce significant variation in the probability of detecting porpoises. Here, we hypothesise that changes in porpoise behaviour will drive changes in detection probability. We test this hypothesis by performing a metanalysis of movement and acoustic data collected on 22 harbour porpoises equipped with multi-sensor recorders (DTAGs) in the Kattegat and Belt Seas in Denmark ([Wisniewska et al., 2016](#); [Rojano-Doñate, 2020](#)). We then use a simulation-based method inspired by [Ward et al. \(2008\)](#) but employ simulated recorders instead of a bottom mounted array to estimate detection probability and, thus, quantify the influence of behavioural states on the probability of detecting harbour porpoise clicks on acoustic monitoring devices.

II. METHODS

Calculating the probability of detection from harbour porpoise tag data involved three broad analysis tasks: (1) extraction and analysis of the acoustic and movement data from the DTAGs, (2) quantifying the different behavioural states from the tag data, and, finally, (3) building a

simulation to model the probability of detection for different behavioural states. Factors such as SL, cue rate, or movement while diving extracted from tag data were then modelled as a function of behavioural state to assess how behavioural state could drive changes in probability of detection.

A. DTAG data

Twenty-two harbour porpoises were successfully tagged with suction cup sound and movement recording tags between 2012 and 2019 in the Kattegat and Belt Seas (Denmark). The tagged porpoises were all incidentally caught in pound nets during commercial fishing operations and then tagged and released back into the wild after being assessed as healthy by a specialist. Tags were attached around 5 cm behind the blowhole via four suction cups and detached passively after 6 to 43 h of recording, and recovered by VHF tracking. Handling and tagging of wild porpoises were performed under permission issued to J.T. by the Danish Forest and Nature Agency (SNS-342-00042) and the Animal Welfare Division (Ministry of Justice, 2010/561-1801) during 2012–2014 and from the Environmental Protection Agency (Ministry of Environment and Food of Denmark, NST-3446-0016) and the Animal Experiments Inspectorate (Ministry of Environment and Food of Denmark, 2015-15-0201-00549) during 2015–2019.

Porpoises were tagged with a DTAG-3 or DTAG-4. DTAGs sampled 16-bit stereo (DTAG-3) or mono (DTAG-4) audio at 500 or 576 kHz, respectively, with clip levels between 180 and 190 dB re 1 μ Pa. Each DTAG also contained triaxial accelerometer and magnetometer and pressure sensors (sampled at 250–625 Hz with 16-bit resolution). DTAG-4s were equipped with a fast-acquisitioning Global Positioning System (GPS) sensor, allowing the location of porpoises to be determined when they surfaced.

1. Movement data

Using the DTAG toolbox for MATLAB (MathWorks, Natick, MA),¹ pressure data were converted to depth (m) and, along with magnetic field (μ T) and acceleration ($m s^{-2}$) data, decimated to a common sampling-rate of 25 Hz. A sensor fusion algorithm was used to calculate heading (horizontal angle), pitch (vertical angle), and roll from the accelerometer and magnetometer data streams ([Johnson and Tyack, 2003](#)).¹

GPS data were unpacked and calibrated, and georeferenced three-dimensional (3D) tracks were calculated via a dead reckoning algorithm. For the DTAG-3s, the forward speed was assumed to be $2 ms^{-1}$, and then depth, heading, and pitch data were used to generate a 3D track, starting from the tagged location of the porpoise. This will be very inaccurate as it is based solely on orientation sensor data and an assumption of speed; however, it served as a useful approximation for subsequent analysis of the probability of detecting porpoises, which did not require accurate latitude

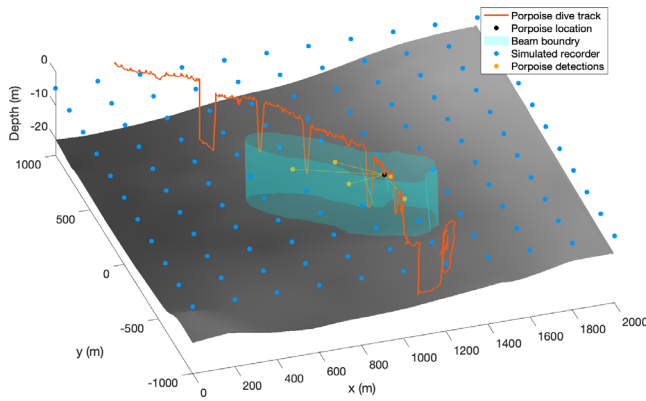


FIG. 1. (Color online) An example of the simulation for the probability of detection. A grid of simulated receivers is placed at a uniform depth of 5 m around the dive track of a tagged porpoise. For every click along the dive track (orange), the SL, orientation, and depth of the porpoise can be used to calculate a received level on every simulated receiver. Here, the beam of a single click, emitted at the position indicated by the black dot, is visualised as a beam volume, i.e., the volume in which the received level is always above a certain threshold (in this case, 100 dB re 1 μ Pa pp). If a receiver is inside the volume (yellow dots), i.e., the received level is above threshold, then it detects the click, and the range to the porpoise is recorded.

and longitude locations (see Sec. II C). The DTAG-4s contained a GPS and, thus, dead reckoning could be recalibrated for every GPS fix, providing much more accurate 3D geo-referenced tracks and allowing tag tracks to be referenced to bathymetry data (primarily for visualisation purposes in Figs. 1 and 2).

2. Acoustic data

Acoustic data recorded on the DTAGs were processed in PAMGuard² and MATLAB (MathWorks, Natick, MA) to automatically extract all focal clicks (direct path clicks from the tagged animal). PAMGuard’s click detector module was initially used to detect all transients 10 dB above in-band noise (Chebychev 100–200 kHz bandpass, fourth-order), including focal and non-focal porpoise clicks and random transient noise. The focal clicks detected on a DTAG are recorded only a few centimetres from the sound source, and the waveform is significantly distorted with the majority of energy between 150 and 200 kHz (Madsen *et al.*, 2010) in comparison to the typical range from 110 to 150 kHz observed for clicks recorded some distance from porpoises, including surface reflections and clicks from conspecifics. These unique off-axis spectra meant that it was possible to automatically detect focal clicks using PAMGuard’s automated click classifier combined with a MATLAB (R2021b, MathWorks, Natick, MA) script to remove remaining false positives. Buzzes and communication click trains were then identified as sections of focal clicks with an inter click interval (ICI) < 16 ms (Wisniewska *et al.*, 2016; Sørensen *et al.*, 2018). The results from the automated classification were compared to a subset of manually annotated data (a random 10-min period for ten tags) with results showing a relatively high accuracy [recall = 0.96/0.95, precision = 0.96/0.99 (click/buzz); see the supplementary material³].

The hydrophones of all available DTAGs were calibrated against a pre-calibrated TC4013 hydrophone

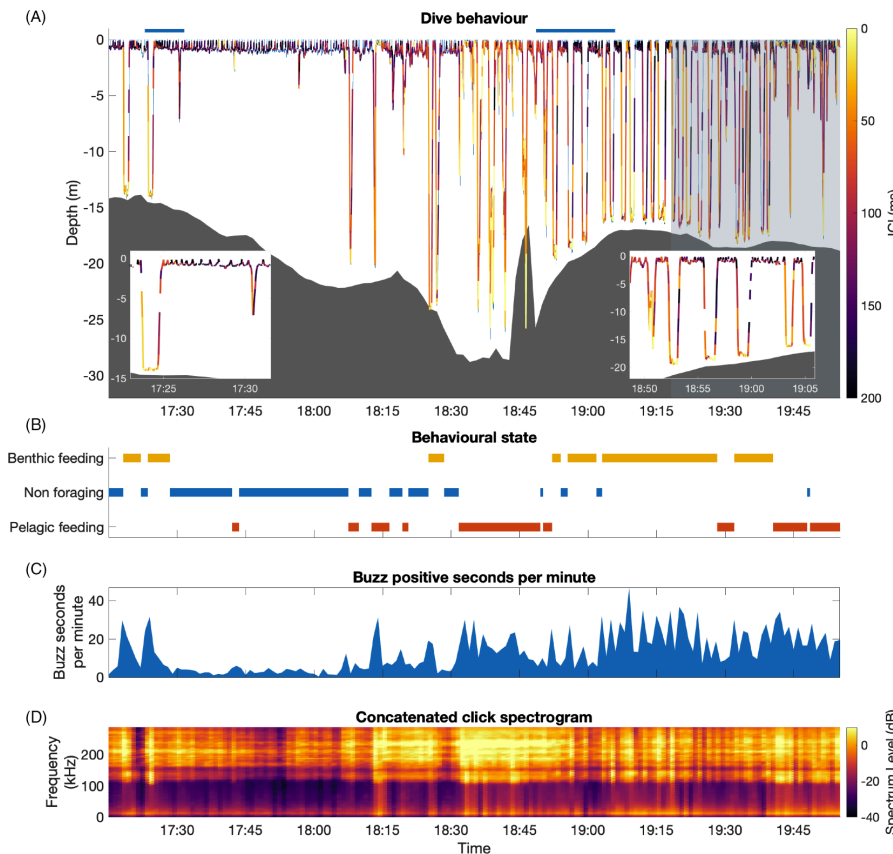


FIG. 2. (Color online) A 3-h example of DTAG-4 data from a tag deployment (hp17_135a) with GPS, which allows for the matching of bathymetry data. Dive profiles coloured by ICI are displayed in (A) along the corresponding depth of bathymetry (dark gray). The shaded light gray background represents nocturnal periods. Two depth profile insets (time is highlighted by the two blue lines on top of the dive profile) appear zoomed in examples of diving behaviour. The left inset shows a single dive of benthic foraging followed by non-foraging behaviour, and the right inset shows pelagic and benthic foraging. (B) shows the estimated behavioural states of the porpoise over the 3-h period: benthic foraging (yellow), non-foraging (blue), and pelagic feeding (red). (C) is the number of seconds that contain a buzz per minute—larger values likely indicate increased foraging activity. (D) shows the average spectra of all focal clicks in 10 s bins.

(Teledyne RESON A/S, Slangerup, Denmark). Some DTAGs were later lost at sea during subsequent deployments or, otherwise, unavailable for calibration; previous calibration information or the mean calibration of the same model of DTAG were used in this case (see the supplementary material³).

B. Behavioural state data

Dives recorded on the DTAGs were classified into three behavioural states (non-foraging, pelagic feeding, and benthic feeding) using a hidden Markov model based on eight dive metrics selected to reflect the movement and activity of harbour porpoises (Rojano-Doñate *et al.*, 2020). Non-foraging dives had few or no buzz detections, pelagic feeding occurred when buzzes were distributed throughout the dive, and benthic feeding occurred when buzzes were primarily recorded near the maximum dive depth. As described in Rojano-Doñate (2020), dives during various behavioural states differed in duration and maximum depth, as well as in the number of buzzes. While bottom feeding dives were the longest and deepest dives, there were, on average, more buzzes during pelagic feeding dives.

C. Modelling detection probability

There are two commonly used methods for calculating animal density from static recording devices. The first method is cue counting, where the probability of detecting a single vocalisation is used to estimate density via

$$\hat{D} = \frac{n_c(1 - \hat{f}_c)}{a_c \hat{P}_{click} T \hat{c}}, \tag{1}$$

where n_c is the number of detected cues (clicks in this case), \hat{f}_c is the estimated proportion of false positives, a_c is the maximum area covered by the instrument (taken to be a circle with a radius of the maximum detection range), \hat{P}_{click} is the average probability of detecting a cue in the area a_c , T is the total time spent monitoring, and \hat{c} is the average cue rate per animal in clicks per unit time of T (Marques *et al.*, 2013).

The second method, often referred to as the snapshot method, involves dividing the survey effort into short sequential snapshots, where animal movement within a snapshot is assumed to be insignificant. The probability of detection then becomes the probability of detecting a group (an animal or animals) within a snapshot rather than the probability of detecting a single cue (click); density using the snapshot approach is calculated as

$$\hat{D} = \frac{n_s(1 - \hat{f}_s)g}{a_c \hat{P}_{snap} T_s}, \tag{2}$$

where n_s is the number of snapshots which register a detection, \hat{f}_s is the estimated proportion of false positive snapshots, g is the average group size, \hat{P}_{snap} is the average probability of detecting a porpoise(s) within a snapshot, and

T_s is the total number of snapshots. Note that the snapshot approach does not require a cue rate, but instead an estimate of the average group size (g) is required, i.e., the average number of individual animals detected within a snapshot. There are numerous ways that g can be calculated, for example, by considering data from visual surveys. Because cue rate is a difficult parameter to determine without acoustic tag data, the snapshot approach in Eq. (2) can represent a more analytically feasible approach to density estimation. However, within the time period of a snapshot (here 1 s—see Sec. IID), an animal might produce multiple vocalisations; the rate and direction of these will influence the probability of detecting a snapshot, introducing an additional behavioural component to \hat{P}_{snap} . As such, \hat{P}_{snap} may be more sensitive to changes in animal behaviour than \hat{P}_{click} .

For a PAM survey, the two typical unknowns are the probability of detecting a click (\hat{P}_{click}) and the cue rate (\hat{c}) in Eq. (1) and the probability of detecting a snapshot (\hat{P}_{snap}) and the group size (g) in Eq. (2). Calculating the average cue rate (\hat{c}) from tags is straightforward; it is simply the total number of focal clicks detected on the tag divided by the total time the tag was on the porpoise. Group size (g), however, is much less practical to calculate from tag data and, thus, considered an unknown for the remainder of the paper.

Calculating \hat{P}_{click} or \hat{P}_{snap} using DTAG data requires that the received levels from a focal click can be accurately estimated on a simulated recorder at a specified location. Each DTAG provides the 3D tracks, orientation, acoustic behaviour, and apparent output level of a harbour porpoise. To be able to calculate the received level of a click on a recorder at a specified location from an animal requires three additional pieces of information: (1) the on-axis SL, (2) the full spherical beam profile of the animal, and (3) acoustic propagation conditions. If these are known, the received level on a recorder at (x,y,z) m from the porpoise is calculated via

$$RL = ASL - TL, \tag{3}$$

where RL is the received level on the recorder, ASL is the apparent source level (Møhl *et al.*, 2000), and TL is the transmission loss. $ASL = SL - BL$, where SL is the on-axis SL of a click, and BL is the beam loss due to the beam profile, which is a function of the relative horizontal and vertical angles between the centre of the acoustic axis of the porpoise and the recorder. TL depends on acoustic propagation and absorption, which is a function of the range and depth of the recorder and porpoise, frequency of the clicks, and oceanographic conditions such as salinity, temperature, pH, and depth (DeRuiter *et al.*, 2010).

Once the received level on a recorder can be accurately calculated, then the probability of detecting a harbour porpoise click can be estimated using a simulation. Simulated recorders were placed in a 100m grid at 5m depth (to account for the fact that much of Kattegat and the Belt Seas are shallow) up to a distance of 1200m around the dive

track of the porpoise (see Fig. 1). For each focal click, RL was calculated for all recorders. If RL was above a defined detection threshold (100 dB re 1 μ Pa pp in this case—see the supplementary material³), then the received click was considered detected. Because the simulated recorders are evenly distributed with respect to the dive track (they are in a regular grid), then the key distance sampling assumption of evenly distributed animals is valid and, thus, the number of detected clicks divided by total number of received clicks (within 1200 m) is an estimate of the probability of detection. Similarly, a probability density function (\hat{P}_{click} or \hat{P}_{snap} at different ranges) can be generated by binning detected and received clicks by range. For the snapshot approach, the simulation is exactly the same except the probability of detection is calculated as the number of receivers that detect at least one click within the snapshot period divided by the total number of receivers. Note that the maximum distance of 1200 m used in the simulation is arbitrary—increasing the distance will lower the overall probability of detection (because a larger area is being considered), but this is compensated for in the overall density estimate by an increase in a_c in Eqs. (1) and (2). Current estimates suggest that porpoise clicks can be detected up to 1000 m (DeRuiter *et al.*, 2010) and, hence, 1200 m maximum range represents a liberal estimate likely to encompass all detectable animals.

The accurate calculation of the probability of detection is predicated on the accurate calculation of *SL*, *BL*, and *TL* for each focal click. These were determined as follows.

1. SL

On-axis SL was calculated from the apparent output level (i.e., the received level of focal clicks on the tag) by comparing SL and apparent output level from previous experiments on captive animals tagged with a DTAG-4 while simultaneously being recorded from a few metres ahead of the swim path (Ladegaard and Madsen, 2019). This provided a ballpark relationship between SL and the apparent output level recorded on the tag, however, there were still significant unknowns around how tag placement and apparent output level varies between animals; thus, these SL values were considered an estimate rather than precise values (see the supplementary material for details³).

2. BL

For any given click, the position and orientation (from tag data) of the porpoise and location of the simulated recorder are known. The position and horizontal and vertical orientation of the porpoise can be used to calculate relative horizontal and vertical angles between the porpoise and receiver. BL could then be extracted from the full spherical beam profile measured in a captive harbour porpoise (Macaulay *et al.*, 2020, which also contains additional details about calculating relative angles).

3. TL

The Kattegat and Belt Seas are shallow areas leading to multipath propagation, and temperature and salinity gradients, which are capable of refracting narrow-band high-frequency clicks (DeRuiter *et al.*, 2010). Thus, there is potential for distortion of the acoustic field around a harbour porpoise. Although DTAGs have a temperature sensor, they do not record salinity, and high-resolution data on bathymetry and bottom type is not available in most locations; thus, accurately estimating multipath and refracted propagation was not feasible. A simple spherical spreading model was, therefore, used to estimate TL:

$$TL = 20 \log_{10}(R) + \alpha R, \quad (4)$$

where R is the range between a porpoise and the recorder, and α is the absorption coefficient for a click in dB/m, which was estimated to be 0.04 dB/m based on a peak frequency of 130 kHz for on-axis clicks (Ainslie and Mccolm, 1998).

Although this estimation of TL is an oversimplification, previous experiments have shown that even in situations where there are strong temperature and salinity gradients, spherical spreading is still a good approximation with less than 3 dB error at ranges up to 200 m at most study sites (DeRuiter *et al.*, 2010).

D. Simulation processing

Buzz clicks were removed from the data before running the simulation partly because buzz clicks have very low SLs and, hence, little PAM relevance and partly because the beam profile of a buzz click is significantly wider than that of non-buzz echolocation clicks (Wisniewska *et al.*, 2015; Malinka *et al.*, 2021). Thus, the relative amplitudes of buzzes and clicks do not reflect the on-axis relative amplitudes, which would have introduced a bias into the probability of detection.

The data from all tags was combined and then split into three different behavioural states and diurnal/nocturnal periods. A simulation was next run for each combination of behavioural state and diurnal/nocturnal period (a total of six simulations in total). The subsequent simulation results (i.e., the number of detected clicks divided by the total number of clicks within 1200 m of each simulated device) were then direct measurements of the probability of detection of the tagged harbour porpoises during different behavioural states and diurnal/nocturnal periods. The simulations were run for individual clicks to calculate \hat{P}_{click} and 1-s snapshots to calculate \hat{P}_{snap} —note that the 1-s time was chosen as this was the value used in the SAMBAH project, the largest static PAM study to date (Amundin *et al.*, 2022).

The probability of detection for each tag for different behavioural and diurnal states was then compared by considering the ratio in \hat{P}_{click} or \hat{P}_{snap} between behavioural states and/or diel periods. A ratio, rather than absolute values, was used because the probability of detection scales with SL (see the supplementary material³) and measuring

SLs from tags is likely an unstable measurement. Therefore, the ratio of \hat{P}_{click} or \hat{P}_{snap} between behavioural states provides a better comparison between different tags.

E. Data exploration and modelling

The simulations provide an estimate of \hat{P} but no insights into the behavioural drivers behind changes in the probability of detecting animals. \hat{P} may be influenced by a large number of potential behavioural and environmental factors such as the horizontal dive angle, depth distribution, SL, beam profile, propagation conditions, etc.

For each second and each tag, we modelled the following response variables: (1) median SL (dB re $1 \mu\text{Pa}$ pp at 1 m), (2) change in vertical dive angle ($^\circ$), (3) change in horizontal angle of DTAG orientation sensors to infer scanning behaviour, and (4) the number of clicks produced as a measure of cue rate. Generalized linear mixed models (GLMM) were used to investigate whether SL, cue rate, or vertical and horizontal angle change varied as a function of the previously identified behavioural states and diurnal/nocturnal periods. Significant changes in these metrics are interpreted and discussed in terms of the potential changes in \hat{P} —see Sec. II C).

To account for the dependent nature of data and consecutive measurements over time, coming from the same animal and the same dive, all models included animal identification (ID) and dive ID as random intercepts. Additionally, models included behavioural state as random slope as a function of animal ID. The need to include an autoregressive covariance structure to account for the temporal autocorrelation and a variance structure to correct for potential heterogeneity of the residuals between different behavioural states and animal IDs was checked by plotting the autocorrelation function and residuals for each model and comparing the corresponding Akaike information criterion (AIC) and were not deemed necessary for any of the models. A Gaussian family was used for the models with SL and vertical dive angle as response variables, a Beta distribution limited between 0 and 180 for the change in horizontal angle, and a quasi-Poisson family with zero-inflation when modelling number of clicks. The statistical analysis was performed in *R* software (version 4.1.2; R Core Team, 2021), using the *lme* function of the *nlme* package (version 3.1–153; Pinheiro *et al.*, 2021), and the *glmmTMB* function of the *glmmTMB* package (version 1.1.2.3; Brooks *et al.*, 2017).

III. RESULTS

A. Example DTAG data

Figure 2 shows an example of the acoustic and behavioural data collected on a DTAG-4. The concatenated spectrogram [Fig. 2(D)] shows the distorted spectra of focal clicks received by a DTAG deployed on a harbour porpoise; the click spectra are summed for each time bin and, therefore, increasing or decreasing intensity indicates either changes in SL or the number of clicks per unit time. Dive

behaviour and ICI relate to changes in the behavioural states [Fig. 2(A)] with porpoises switching from mostly non-foraging activity $\sim 18:15$ h to pelagic and benthic foraging with a decrease in average ICI.

B. Meta-analysis of DTAG data

Across all tags, porpoises produced a median of 21 299 (25% and 75% percentile, 11 840 and 26 383, respectively) clicks per hour during daylight and 27 925 (25% and 75% percentile, 22 964 and 35 583, respectively) clicks per hour during darkness. A summary of the ICI, SL, vertical dive angle, and depth distribution during diurnal and nocturnal periods for four example DTAG deployments is shown in Fig. 3 (a summary for all tags is available in the supplementary material³). The distribution of ICI is depicted at several scales, corresponding to the typical ICIs during buzzing, non-buzz echolocation behaviour, and over a 0–60 s scale to demonstrate silent periods. Note the similarity in the distributions between different animals during buzzing and non-buzzing echolocation behaviour—however, the silent periods are much more variable. SLs also vary considerably between individuals with some individuals producing considerable numbers of clicks estimated to be above 200 dB re $1 \mu\text{Pa}$ pp at 1 m (see Sec. II C 1). Most animals spend the majority of time in the upper 5 m of the water column, but dive behaviour below this was highly varied with some porpoises showing a strong bimodal distribution, which likely indicates benthic foraging (e.g., hp18_274a). The bathymetry also varied considerably among deployments. For example, hp18_134a was tracked diving to 80 m in the Kattegat Sea while the maximum dive depth of hp17_135a was 27 m, and it never entered waters deeper than 30 m.

C. Behavioural states

The behavioural states for all tag deployments are shown in Fig. 4. Although the behavioural states with respect to time of day vary considerably between different animals, there is a discernible trend toward pelagic feeding during nocturnal periods (26% day and 59% night) and more of non-foraging (51% day and 26% night) and benthic feeding (23% day and 15% night) periods occur during daylight hours (sensu Rojano-Doñate, 2020).

D. Probability of detection simulation

DTAG deployments were broken into segments based on behavioural state and diel period; the input for each simulation was then the segment from one behavioural state and diel period, resulting in a total of six simulations (three behavioural states for both diurnal and nocturnal periods). Figure 5 shows tag hp17_135a (DTAG-4) as an example of the probability density function (i.e., the proportion of detected clicks with range) for single clicks and snapshots, during nocturnal and diurnal periods, and for different behaviours. A probability density function assumes an even distribution of animals around a device [i.e., the area under the graph is a direct calculation of \hat{P}_{click} or \hat{P}_{snap} for Eq. (1)

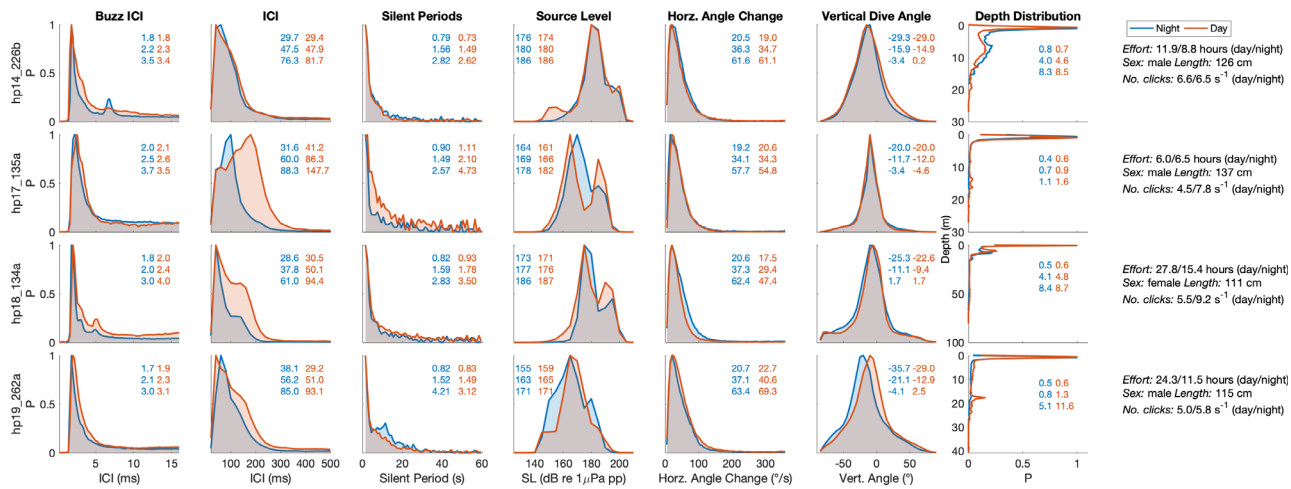


FIG. 3. (Color online) An example of the meta-analysis of 4 of 22 tagged harbour porpoises. Each row shows the buzz ICI (<16 ms), ICI (between 16 and 500 ms), silent periods (>0.5 s), SL, vertical dive angle, horizontal angle change (the maximum change in horizontal angle in a 1 s period), and depth distribution of a tagged animal during diurnal (orange) and nocturnal periods (blue). Effort, sex, animal length, and cue rate (clicks per second) are also displayed at the end of each row. The text in each plot is 25th, 50th, and 75th (top, middle, and bottom, respectively) percentiles for each diurnal (orange) and nocturnal (blue) period.

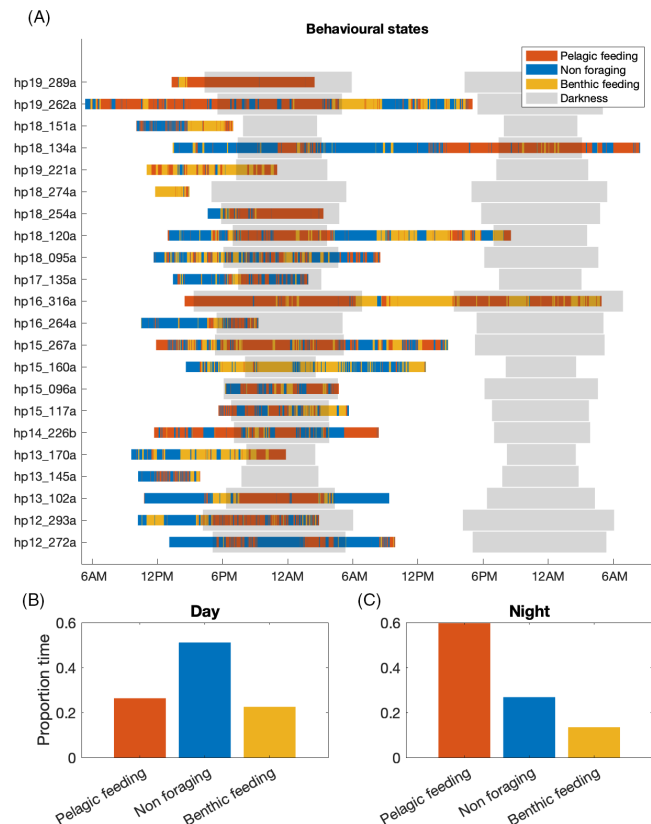


FIG. 4. (Color online) (A) shows the behavioural states of all tagged porpoises with time of day (pelagic feeding, red; non-foraging, blue; Benthic feeding, yellow). Hours of daylight are white and darkness are plotted as semi-transparent gray boxes, which vary in size from animal to animal depending on the time of year of the tagging. The start and end of the deployment times vary between porpoises because animals were tagged at different times of day, and the total time a suction cup tag stays on an animal varies considerably. (B) and (C) show the relative time spent in each behaviour state during the diurnal and nocturnal periods, respectively.

or (2), respectively]. For a static recording device, the number of animals increases linearly with increasing range, e.g., there are nine times more animals between 200 and 250 m than between 0 and 50 m because the area between 200 and 250 m is nine times larger. Thus, at shorter ranges, where the probability of detecting an individual porpoise is relatively high, the probability density function increases with range because it is dominated by the increasing number of animals at greater ranges. At larger ranges, the probability of detecting an individual porpoise begins to decrease significantly and, thus, the probability density function reaches a peak and begins to fall as the dominant factor becomes the decreasing chance of detecting the clicks of an individual animal. Note that in all probability density functions here, there is a steep initial peak; this is because at closer ranges, harbour porpoises can be detected at most orientations due to low amplitude off-axis acoustic energy. As range increases, only the click energy within a porpoise's anteriorly directed and narrow beam is detectable (Macaulay *et al.*, 2020).

Figure 5 demonstrates that there is little difference between the overall probability of detecting a single click (\hat{P}_{click}) for different behavioural states and diurnal and nocturnal periods. However, the opposite is true for the snapshot approach, where there are large behavioural differences in \hat{P}_{snap} , and these vary significantly between foraging states and nocturnal and diurnal periods. This pattern is broadly repeated across all tags. Figure 6 shows a summary of the ratio of \hat{P}_{click} or \hat{P}_{snap} for pelagic and benthic foraging compared to non-foraging states. The median difference (day and night) in \hat{P}_{click} between different behavioural states is <30%; however, for the snapshot approach (\hat{P}_{snap}), the median difference is between 274% and 330%.

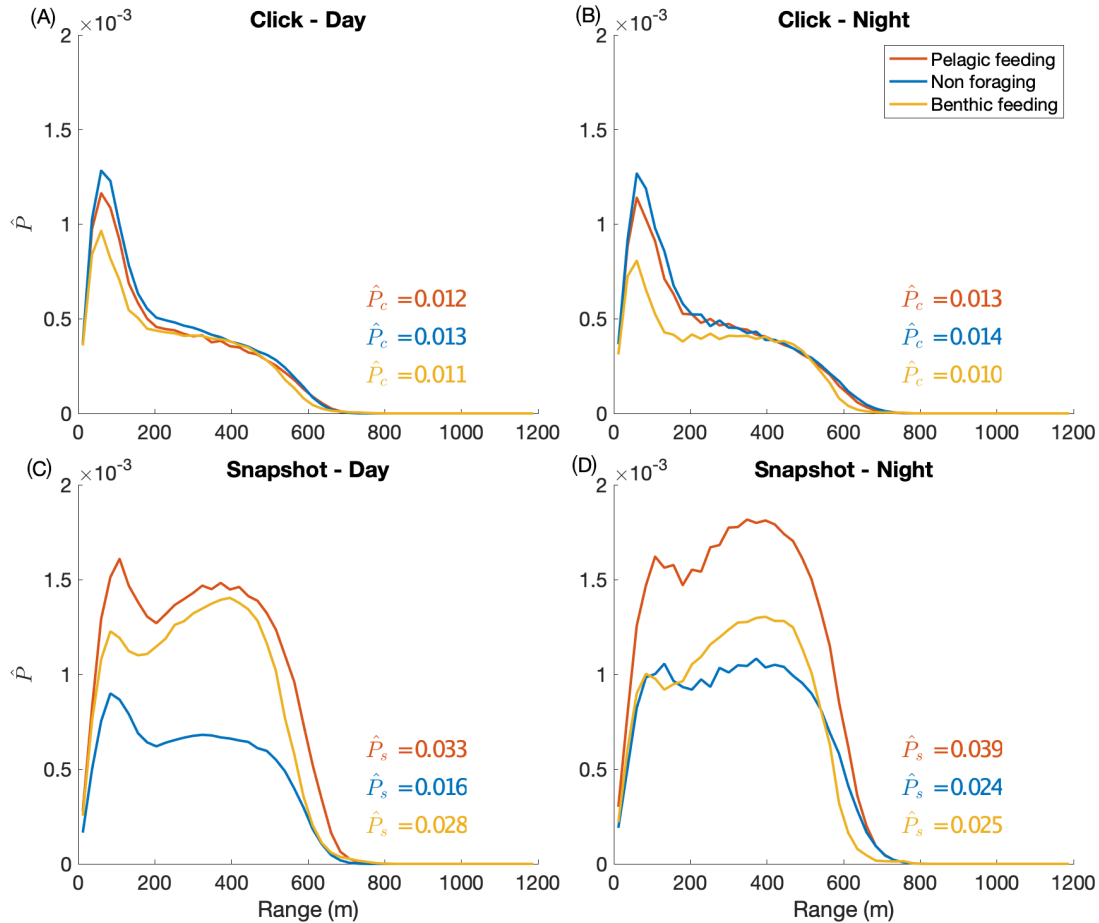


FIG. 5. (Color online) Probability density functions for individual clicks and snapshots over different behavioural and diel periods generated by the probability of detection simulation for tag hp17_135a. (A) and (B) (day/night) show the probability density function for an individual click, and (C) and (D) (day/night) show the probability density function for a 1-s snapshot. In all plots, the probability density is represented as a function of three behavioural states (pelagic feeding, red; non-foraging, blue; benthic feeding, yellow). The average probability of detection for an animal within 1200 m for each behavioural state is shown as corresponding coloured text. The probability of detecting an individual click [(A), (B)] is relatively stable; however, the probability of detecting a snapshot [(C), (D)] varies considerably with respect to different behavioural states and diel period.

When comparing the probability of detection between diurnal and nocturnal periods, the median \hat{P}_{click} for each of the three behavioural states is lower at night (pelagic foraging, -15% ; non-foraging, -9% ; benthic foraging, -41% ; Fig. 7). Median \hat{P}_{snap} is also lower at night during pelagic (-12%) and benthic (-25%) foraging but higher during non-foraging ($+32\%$). Overall, changes in \hat{P}_{snap} between day and night are significantly less than the change in \hat{P}_{snap} between different behavioural states.

E. Click parameters as a function of behavioural state and diel period

The much larger changes in \hat{P}_{snap} with different behavioural states compared to \hat{P}_{click} are most likely the result of specific behaviours significantly altering the chances that at least one click is detected within a snapshot window. The simulation provides no information on the mechanism that drives this disparity; however, the results from modelling changes in cue rate, SL, and scanning behaviour (the maximum horizontal angle change in 1 s) provide a potential explanation.

Figure 8 shows a summary of the raw data distributions and model result estimates of SL (dB re $1 \mu\text{Pa}$ pp at 1 m), maximum change in horizontal angle ($^\circ$), vertical dives angle ($^\circ$), and the number of clicks in 1-s bins for all tags during different diurnal/nocturnal periods and behavioural states. Overall, SL and cue rate are strongly associated with behavioural state (particularly between non-foraging and pelagic/benthic foraging states) with a much weaker relationship with diel state. However, horizontal and vertical angle changes remain broadly stable with a slight consistent decrease during regular clicking periods at night. Corresponding detailed model results are available in the supplementary material.³

IV. DISCUSSION

The probability of detecting a harbour porpoise is a key metric in converting acoustic data into non-biased estimates of animal abundance, habitat use, and effects of human activities at sea. Here, we used a large tag dataset to explore the merits of two approaches to density estimation: detection of individual clicks (\hat{P}_{click} , click counting) and detecting at

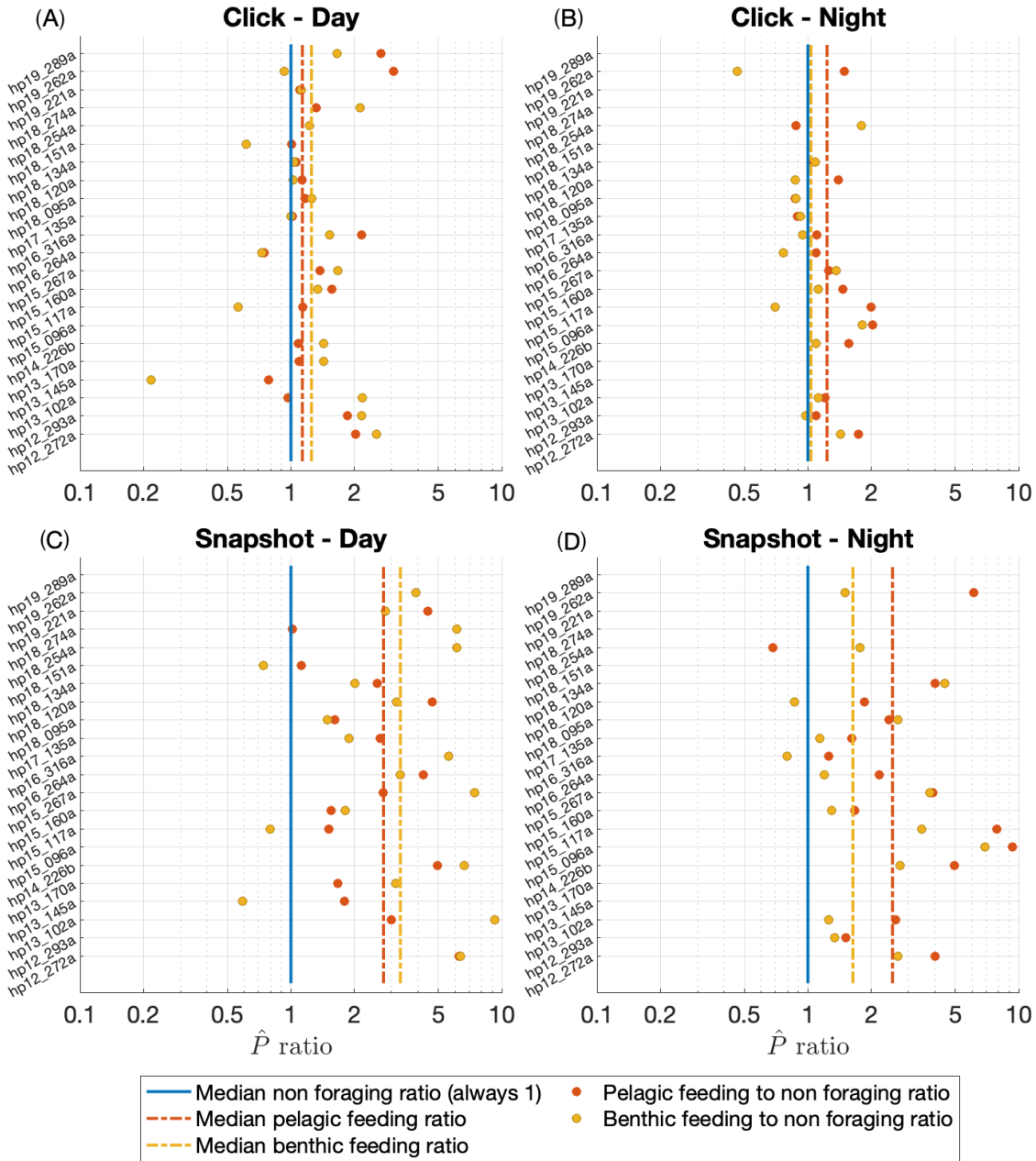


FIG. 6. (Color online) The ratio in the probability of detection between non-foraging and foraging states for all tags using non-foraging as reference. The vertical lines show the median ratio for each behavioural state (note that non-foraging will always be one). (A) and (B) (day/night) show the ratio of \hat{P}_{click} and (C) and (D) (day/night) show the ratio of \hat{P}_{snap} . The ratio between foraging and non-foraging states for \hat{P}_{click} is close to one during diurnals and nocturnal periods, whereas the ratio for snapshots is highly dependent on foraging state and diel period, varying by up to a factor of 4, on average, but up to factor of 10 in some specific animals. Note the ratio axis is logarithmic.

least one click within a 1-s time window (\hat{P}_{snap} , snapshot). We found that behavioural state had a substantial impact on detectability with clicking rate (cue rate) and \hat{P}_{snap} significantly increasing during benthic and pelagic foraging compared to non-foraging behaviour. In contrast, diel state had less influence on detectability, where \hat{P}_{snap} and \hat{P}_{click} slightly reduce for different behaviours and have no consistent influence on click rates during nocturnal periods. However, diel state does have a significant *overall* effect on detectability because porpoises forage more at night (Fig. 4), and foraging behaviours are significantly more detectable; porpoises

are, therefore, broadly more detectable at night. Thus, behavioural state (which changes with diel state) predominantly drives the average clicking rate and \hat{P}_{snap} during PAM studies with significant downstream consequences for interpretation of PAM studies, which use cue counting or snapshot approach methods.

A. Why are \hat{P}_{snap} and \hat{P}_{click} different?

The probability of detection for a snapshot (\hat{P}_{snap}), i.e., the probability that at least one click was detected within a

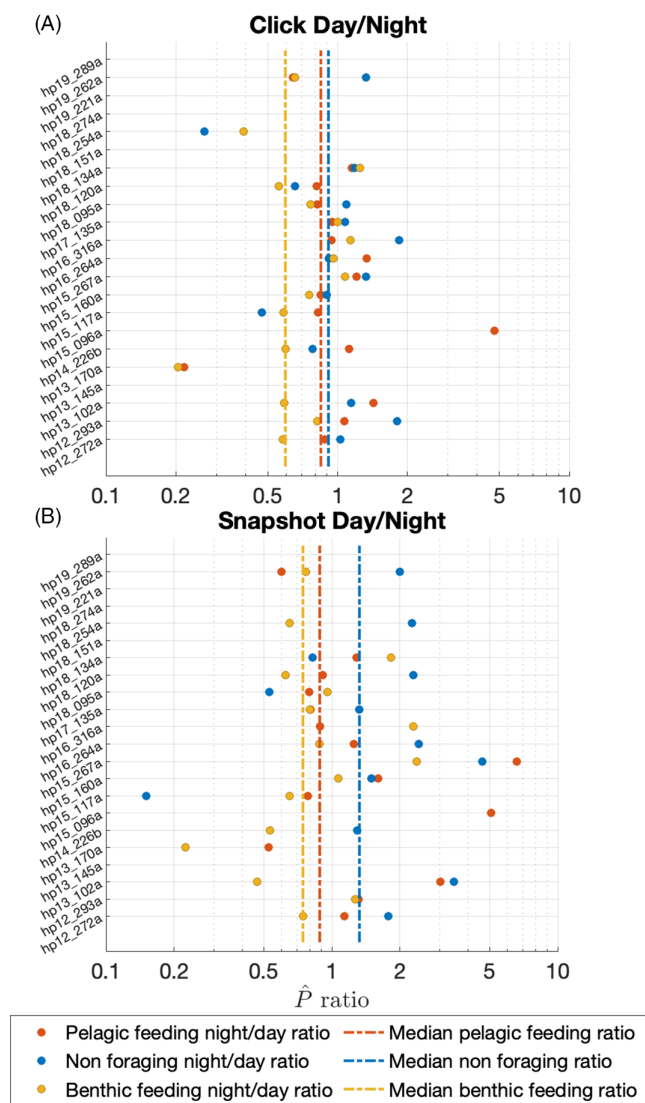


FIG. 7. (Color online) The ratio of the probability of detection between diurnal and nocturnal periods for each tag deployment over different behavioural states using diurnal periods as a reference. (A) shows the ratio between the probability of detection for a single click, and (B) depicts the probability of detection ratio for a snapshot. The dashed lines show the median ratio for each behavioural state (pelagic feeding, red; non-foraging, blue; benthic feeding, yellow).

1-s period, varied considerably with behaviour and diel period, whereas the probability of detecting individual clicks (\hat{P}_{click}) remained relatively stable across behavioural and diel states (Fig. 6). This is because \hat{P}_{snap} considers the auto-correlation between successive clicks within a snapshot. Detection of a single click depends on the click itself (the amplitude) but also on the orientation of the porpoise relative to the PAM recorder and is independent of the preceding or following clicks in a sequence. For detection in a snapshot, this is different because the change in behaviour from one click to the next affects the probability that at least one click is detected within the snapshot period. For example, consider a porpoise that is clicking and scanning (moving the head side to side) rapidly. Its highly directional beam profile means that as it scans, it will ensonify many

more sensors than if it were moving slowly in a fixed direction and clicking slowly. If the same scenario is considered for an individual click, assuming that the depth and vertical orientation remains the same, then probability of detecting an individual click is unaffected by an animal turning or how rapidly it is clicking (see Fig. 9). Thus, scanning behaviour and click rates will significantly influence the probability of detecting a click within a snapshot but not an individual click. The 1-s snapshot chosen here (because it was used in the SAMBAH project; Amundin *et al.*, 2022) is clearly long enough for scanning behaviour and click rates to have a significant impact on \hat{P}_{snap} . However, a 1-s snapshot represents a compromise between minimising movement effects and preventing significant temporal correlation, i.e., if the size of a snapshot decreases, the potential for multiple clicks and large changes in movement will decrease, but this will introduce additional downstream statistical issues as smaller snapshots become highly correlated over time and most will contain no detections (Marques *et al.*, 2013).

B. What drives the behavioural dependent changes in \hat{P}_{snap} ?

\hat{P}_{snap} decreased slightly for individual behavioural states during nocturnal periods (Fig. 7), however, any associated decrease in overall detectability was negated because proportion of time spent foraging at night greatly increased (Fig. 4, foraging behaviours = 49% during daytime versus 74% at night), and the increase in \hat{P}_{snap} during foraging behaviours (+254% on average) is far higher than the small decrease due to diel state (-25% average). The model results in Fig. 8 provide some indication of why \hat{P}_{snap} increases during active foraging behaviours. Average click rates and SLs increased ($\sim 2-3\times$ and +6 dB, respectively) during pelagic and benthic foraging with a horizontal angle change per second remaining similar between behaviours at around 47–61 deg/s, suggesting animals were consistently actively scanning to search new water volumes for fish. The difference in click rates and SLs between diel periods was negligible in comparison to behavioural influences, suggesting a combination of higher click rates driven by consistent active scanning behaviour (as discussed in Sec. IV A), and increased SLs were the primary driver of the large increases in \hat{P}_{snap} during foraging behaviours. Thus, the simulation (increased \hat{P}_{snap} during foraging), model results (increased click rates during foraging), and distribution of behaviours (Fig. 4, 25% increase in foraging at night) all suggest that the often-observed differences in PAM data between diurnal and nocturnal periods (Schaffeld *et al.*, 2016; Stedt *et al.*, 2023) are not due to changes in acoustic behaviour within individual behavioural states but instead are primarily a consequence of porpoises being more likely to be in a foraging state during nocturnal periods, leading to a higher probability of detection (Fig. 4).

It should be noted that it is primarily the narrow beam profile of harbour porpoises that translates changes in scanning behaviour and cue rate to large changes in \hat{P}_{snap} .

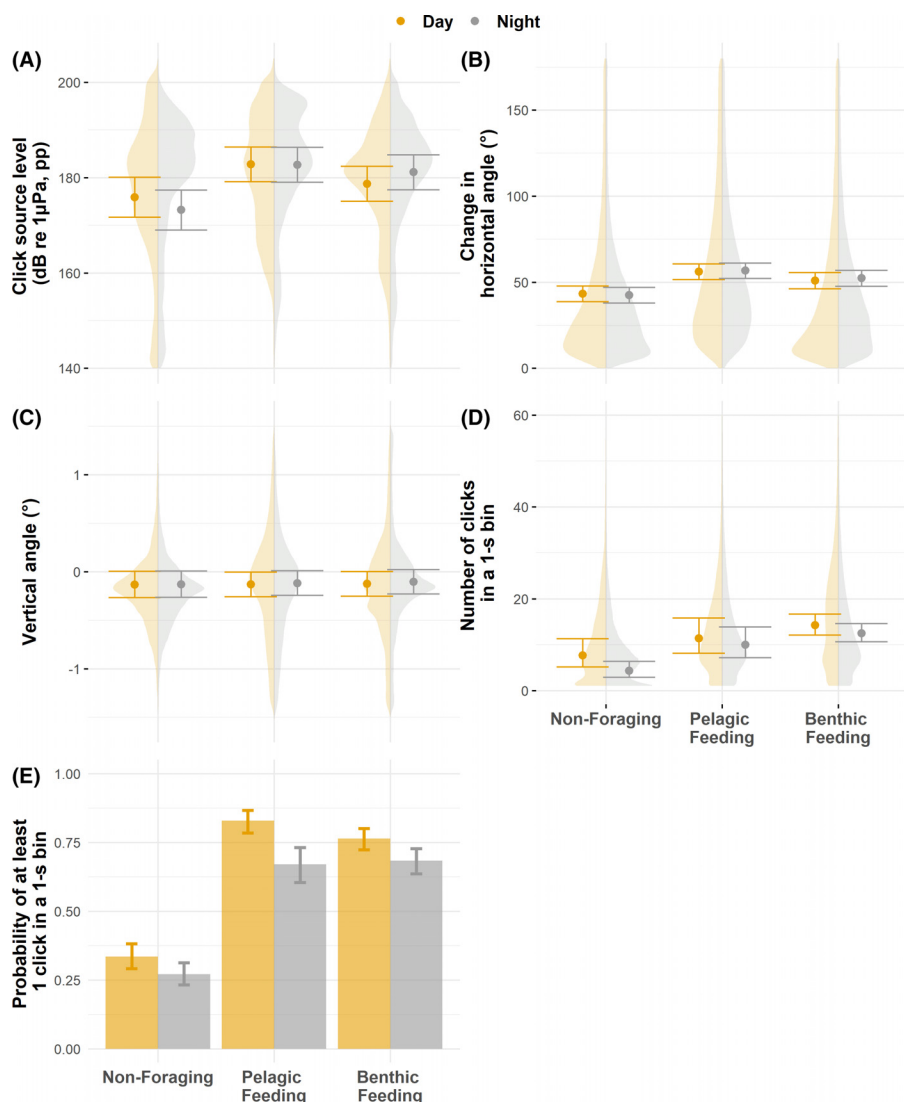


FIG. 8. (Color online) Distributions of SL (A), maximum horizontal angle change in 1 s (B), vertical dive angle (C), the number of clicks per second (inverse of average ICI) (D), and the probability of a porpoise producing at least one click in a 1-s time bin (E). (A)–(D) show the overall distribution [combined day (orange) and night (gray)] of raw data during different behavioural states and for regular clicks (excluding buzzes). The dots and whiskers in all plots represent the mean model estimate and 95% confidence interval for each distribution.

For example, an omnidirectional beam would not result in any change to \hat{P}_{snap} for a rotating or non-rotating animal (see Fig. 9 and the supplementary material³). Consequently, it is reasonable to assume that the behavioural state of other toothed whale species, all of which have similarly narrow beam profiles (Jensen *et al.*, 2018), will also have a significant influence on \hat{P}_{snap} . Conversely, there is, therefore, less influence of behaviour on \hat{P}_{click} or \hat{P}_{snap} for soniferous species which have much *less* directional sound production, such as baleen whale calls and whistles produced by many delphinid species (Blackwell *et al.*, 2012; Branstetter *et al.*, 2012).

C. Implications for future PAM surveys

Abundance estimation is usually predicated on a number of assumptions, and key to an effective survey is understanding how robust these assumptions are. Here, we have shown that the click counting and snapshot approaches to density estimation are based on the same underlying principles, and both can make assumptions that are not fully supported when animals in a given area change behaviours.

The probability of detecting a single click is more stable for different behaviours; however, we demonstrate that cue rate, a key term in Eq. (1), is dependent on behavioural states (Fig. 8). The snapshot approach, on the other hand, does not require knowledge on cue rate, but we nevertheless show that the probability of detecting an animal within a snapshot (\hat{P}_{snap}) also varies considerably with behaviour (Fig. 6).

Differing animal behaviours are not necessarily an issue for abundance estimation if they either average out over the period considered or representative values for \hat{P}_{snap} or average cue rates have been estimated *in situ*. However, a significant bias can occur when \hat{P}_{snap} or average cue rates calculated in one type of habitat (or pooled across habitats) or time period are applied to different habitats and/or different time periods. In a worst-case scenario, this could mean that a PAM device placed in a location or time where porpoises exhibit a particular behaviour (e.g., non-foraging, i.e., passing through the habitat) would potentially detect a significantly lower number of clicks compared to an area where porpoises are pelagic feeding for the same density of animals. Similarly, if the data were divided into snapshots, then there could be many more detected snapshots in an area

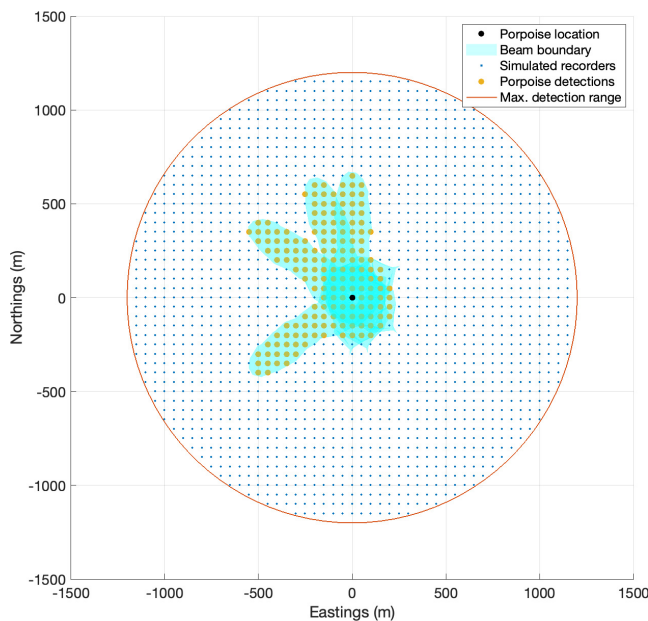


FIG. 9. (Color online) An example of a harbour porpoise clicking four times and turning 125 deg during a snapshot. Each blue point is a simulated PAM device. The translucent area is the beam profile of a porpoise—within this area, the received level is high enough to trigger a detection (yellow points). The probability of detection is the number of triggered recorders divided by the total number of recorders. If the porpoise is turning and clicking rapidly within a snapshot window, then it will ensnare many more receivers—thus, the probability of detecting a snapshot is greatly increased. However, the probability of detecting a click remains almost the same no matter how fast the porpoise is turning or its click rate. If a porpoise were to remain stationary during a snapshot, then the probability of detecting the snapshot and the probability of detecting a single click would be similar [assuming that the received click(s) are always detected].

used for pelagic foraging than in a non-foraging area for the same number of animals. Such errors may lead to incorrect conclusions with downstream implications for research and conservation; for example, it is known that exposure to noise can trigger a switch from foraging to non-foraging behaviour in porpoises (Wisniewska *et al.*, 2018a). A noise effect study could, therefore, detect ~3 times fewer porpoise positive snapshots during a noise exposure experiment for the same distribution and density of animals, leading to the conclusion that two out of three animals leave an area, when, in fact, they may have stayed and changed behaviour, switching from one of energy acquisition to one of energy expenditure; this would imply very different consequences for the fitness of the exposed animals.

The potential bias in density estimation introduced by behavioural states, therefore, has important implications for PAM studies. When collecting acoustic data over large (or possibly relatively small; Stedt *et al.*, 2023) spatial or temporal scales or in situations where animal behaviour might change, it is imperative that there is an understanding of how behavioural states might influence the probability of detection (or cue rate if using a cue counting approach). There is currently no straightforward approach to address the behavioural dependence of \hat{P}_{snap} and cue rates during static PAM studies. It is usually not possible to directly

calculate \hat{P}_{snap} without external experiments, but performing such experiments over sufficient spatial and temporal ranges may be onerous for large-scale surveys and make such studies impractical. Finding the correct balance between pragmatic experimental design for large-scale PAM surveys and minimising bias due to behavioural changes, thus, remains an open question for PAM.

Although difficult to solve, these issues should not be considered intractable; there are several potential research avenues that could be explored to compensate for the behavioural dependence of \hat{P}_{snap} and cue rates. These include carefully considering PAM survey design and the subsequent conclusions that can be drawn from the data, developing classifiers that can determine behavioural states from PAM data and/or adopting the use of PAM devices, which provide some location information (e.g., bearings to clicking animals). These are discussed in more detail in the supplementary material.³

D. Limits of the simulation and future work

The simulation conducted here uses the most accurate behavioural data of harbour porpoises that currently exists to calculate \hat{P}_{click} or \hat{P}_{snap} ; however, despite extensive testing and sanity checks as detailed in the supplementary material,³ it has limitations. The relationship between apparent output level recorded behind the blow hole and on-axis SL of emitted echolocation clicks was determined from trained animals and showed a high degree of variation (see the supplementary material³). Although \hat{P} could be compared across behavioural and diel states, it was not possible to calculate an accurate absolute probability of detection. Additional work is required to assess how sensitive SL calculations are to tag placement and beam width changes (Wisniewska *et al.*, 2015) during clicking and verify whether an accurate on-axis SL of clicks can, indeed, be reliably estimated from on animal recorders.

Also, this dataset only considered animals in primarily shallow waters of the Kattegat and Belt Seas. Porpoises are common in much deeper waters and their behaviour in these environments (e.g., much deeper dives; Nielsen *et al.*, 2019) will almost certainly result in significant changes to the behavioural dependence of \hat{P}_{click} or \hat{P}_{snap} and receiver depths.

In addition, only a very simple criteria for considering positive snapshots (that at least one click must be detected) was used. In reality, many of the devices used in acoustic monitoring of porpoises use click train detectors, which are automated detection algorithms that only register a detection if there is a sequential series of clicks (Sarnocinska *et al.*, 2016). This leads to a complex extra dimension in the probability of detection for click counting and snapshots. For click counting, the probability of detecting a click will be correlated with the number of preceding clicks in a click train sequence. For snapshots, the probability of detection is additionally confounded by the criteria of a click train detector (e.g., the minimum number of clicks to register a

detection), and sequential snapshots shorter than a typical click train may also be autocorrelated. However, such algorithms may also be more robust to different behavioural states because they link multiple clicks over time. Further work is, therefore, required to explore how \hat{P}_{click} or \hat{P}_{snap} are additionally influenced by click train detectors.

V. CONCLUSION

We show that porpoises produce about 0.5×10^6 echolocation clicks per 24 h and their behaviour can have a significant effect on detection probability and click rates, potentially introducing bias into PAM data, particularly between static recorders deployed in different habitats or across different time periods or anthropogenic loads where porpoise behaviour might change. Such behavioural influences may lead to spurious research outcomes and should be carefully considered. Analyses of tag data from natural and disturbed behaviours, the development of classifiers to determine behavioural state from PAM data, technological improvements to monitoring devices, and/or accounting for animal behaviour in survey design provide potential and immediate solutions for future more accurate PAM studies.

ACKNOWLEDGMENTS

We thank colleagues from Aarhus University from the Section for Marine Mammal Research and the Marine Bioacoustics Laboratory, including S. Sveegaard, L. Mikkelsen, M. V. Jensen, R. Dietz, A. Galatius, P. Sørensen, A. Bøttcher, L. Havmøller, L. Bach, J. Balle, E. Iglesias, I. Amirali, F. Larsen, K. Sprogis, S. Videsen, P. Tønnesen, and L. Kyhn, as well as all the helpful fishermen and pilot U. Gosewinkel involved in tag deployments and recoveries. The post-doctoral position for J.D.J.M. was funded by a FNU – Danish Natural Science Research Council grant to P.T.M. This study was also funded by the German Federal Agency for Nature Conservation via the grants “Effects of underwater noise on marine vertebrates” (Cluster 7, Z1.2-53302/2010/14) and “Under Water Noise Effects—UWE” (Project No. FKZ 3515822000). The contribution by T.A.M. was funded under the ACCURATE project (U.S. Navy Living Marine Resources Program, Contract No. N3943019C2176) and CEAL (funded by FCT—Fundação para a Ciência e a Tecnologia, Portugal, through Project No. UIDB/00006/2020). We thank Freja Jakobsen, Kirstin Anderson, and the team at Fjord and Baelt for collecting auxiliary data to calibrate DTAGs. Thanks to Doug Gillespie, Len Thomas, and Danielle Harris (University of St. Andrews) for many conversations about acoustic density estimation.

¹See www.animaltags.org (Last viewed March 11, 2021).

²See www.pamguard.org (Last viewed March 1, 2021).

³See supplementary material at <https://doi.org/10.1121/10.0021163> for a more detailed description of acoustic methods, simulation error, sensitivity checks, and further discussion on possible methods to compensate for behaviourally dependent detectability in PAM studies.

Ainslie, M. A., and McCole, J. G. (1998). “A simplified formula for viscous and chemical absorption in sea water,” *J. Acoust. Soc. Am.* **103**(3), 1671–1672.

Amundin, M., Carlström, J., Thomas, L., Carlén, I., Koblitz, J., Teilmann, J., Tougaard, J., Tregenza, N., Wennerberg, D., Loisa, O., Brundiers, K., Kosecka, M., Kyhn, L. A., Ljungqvist, C. T., Sveegaard, S., Burt, M. L., Pawliczka, I., Jussi, I., Koza, R., Arciszewski, B., Galatius, A., Jabbusch, M., Laaksonlahti, J., Lyytinen, S., Niemi, J., Šaškov, A., MacAuley, J., Wright, A. J., Gallus, A., Blankett, P., Dähne, M., Acevedo-Gutiérrez, A., and Benke, H. (2022). “Estimating the abundance of the critically endangered Baltic Proper harbour porpoise (*Phocoena phocoena*) population using passive acoustic monitoring,” *Ecol. Evol.* **12**(2), e8554.

Andreasen, H., Ross, S. D., Siebert, U., Andersen, N. G., Ronnenberg, K., and Gilles, A. (2017). “Diet composition and food consumption rate of harbor porpoises (*Phocoena phocoena*) in the western Baltic Sea,” *Mar. Mammal Sci.* **33**(4), 1053–1079.

Barlow, J., Fregosi, S., Thomas, L., Harris, D., and Griffiths, E. T. (2021). “Acoustic detection range and population density of Cuvier’s beaked whales estimated from near-surface hydrophones,” *J. Acoust. Soc. Am.* **149**(1), 111–125.

Barlow, J., and Taylor, B. L. (2005). “Estimates of sperm whale abundance in the northeastern temperate Pacific from a combined acoustic and visual survey,” *Mar. Mammal Sci.* **21**(3), 429–445.

Blackwell, S. B., McDonald, T. L., Kim, K. H., Aerts, A. M., Richardson, W. J., Greene, C. R., Jr., and Streever, B. (2012). “Directionality of bowhead whale calls measured with multiple sensors,” *Mar. Mammal Sci.* **28**(1), 200–212.

Börjesson, P., Berggren, P., and Ganning, B. (2003). “Diet of harbor porpoises in the Kattegat and Skagerrak seas: Accounting for individual variation and sample size,” *Mar. Mammal Sci.* **19**(1), 38–058.

Branstetter, B. K., Moore, P. W., Finneran, J. J., Tormey, M. N., and Aihara, H. (2012). “Directional properties of bottlenose dolphin (*Tursiops truncatus*) clicks, burst-pulse, and whistle sounds,” *J. Acoust. Soc. Am.* **131**(2), 1613–1621.

Brooks, M. E., Kasper, K., van Benthem, K. J., Magnusson, A., Berg, C. W., Nielsen, A., Skaug, H. J., Mächler, M., and Bolker, B. M. (2017). “glmmTMB balances speed and flexibility among packages for zero-inflated generalized linear mixed Modeling,” *R J.* **9**(2), 378–400.

DeRuiter, S. L., Hansen, M., Koopman, H. N., Westgate, A. J., Tyack, P. L., and Madsen, P. T. (2010). “Propagation of narrow-band-high-frequency clicks: Measured and modeled transmission loss of porpoise-like clicks in porpoise habitats,” *J. Acoust. Soc. Am.* **127**(1), 560–567.

Jansen, O. E., Michel, L., Lepoint, G., Das, K., Couperus, A. S., and Reijnders, P. J. H. (2013). “Diet of harbor porpoises along the Dutch coast: A combined stable isotope and stomach contents approach,” *Mar. Mammal Sci.* **29**(3), E295–E311.

Jensen, F. H., Johnson, M., Ladegaard, M., Wisniewska, D. M., and Madsen, P. T. (2018). “Narrow acoustic field of view drives frequency scaling in toothed whale biosonar,” *Curr. Biol.* **28**(23), 3878–3885.

Johnson, M. P., and Tyack, P. L. (2003). “A digital acoustic recording tag for measuring the response of wild marine mammals to sound,” *IEEE J. Ocean. Eng.* **28**(1), 3–12.

Koblitz, J. C., Wahlberg, M., Stolz, P., Madsen, P. T., Beedholm, K., and Schnitzler, H.-U. (2012). “Asymmetry and dynamics of a narrow sonar beam in an echolocating harbor porpoise,” *J. Acoust. Soc. Am.* **131**(3), 2315–2324.

Kyhn, L. A., Tougaard, J., Thomas, L., Duve, L. R., Stenback, J., Amundin, M., Desportes, G., and Teilmann, J. (2012). “From echolocation clicks to animal density—Acoustic sampling of harbor porpoises with static dataloggers,” *J. Acoust. Soc. Am.* **131**(1), 550–560.

Ladegaard, M., and Madsen, P. T. (2019). “Context-dependent biosonar adjustments during active target approaches in echolocating harbour porpoises,” *J. Exp. Biol.* **222**(16), jeb206169.

Macaulay, J. D. J., Malinka, C. E., Gillespie, D., and Madsen, P. T. (2020). “High resolution three-dimensional beam radiation pattern of harbour porpoise clicks with implications for passive acoustic monitoring,” *J. Acoust. Soc. Am.* **147**(6), 4175–4188.

Madsen, P. T., Wisniewska, D., and Beedholm, K. (2010). “Single source sound production and dynamic beam formation in echolocating harbour porpoises (*Phocoena phocoena*),” *J. Exp. Biol.* **213**(18), 3105–3110.

Malinka, C. E., Rojano-Doñate, L., and Madsen, P. T. (2021). “Directional biosonar beams allow echolocating harbour porpoises to actively discriminate and intercept closely spaced targets,” *J. Exp. Biol.* **224**, jeb242779.

- Marques, T. A., Thomas, L., Martin, S. W., Mellinger, D. K., Ward, J. A., Moretti, D. J., Harris, D., and Tyack, P. L. (2013). "Estimating animal population density using passive acoustics," *Biol. Rev.* **88**(2), 287–309.
- Marques, T. A., Thomas, L., Ward, J., DiMarzio, N., and Tyack, P. L. (2009). "Estimating cetacean population density using fixed passive acoustic sensors: An example with Blainville's beaked whales," *J. Acoust. Soc. Am.* **125**(4), 1982–1994.
- Møhl, B., Wahlberg, M., Madsen, P. T., Miller, L. A., and Surlykke, A. (2000). "Sperm whale clicks: Directionality and source level revisited," *J. Acoust. Soc. Am.* **107**(1), 638–648.
- Nielsen, N. H., Teilmann, J., and Heide-Jørgensen, M. P. (2019). "Indications of mesopelagic foraging by a small odontocete," *Mar. Biol.* **166**(6), 78.
- Nuutila, H. K., Brundiers, K., Dähne, M., Koblitz, J. C., Thomas, L., Courtene-Jones, W., Evans, P. G. H., Turner, J. R., Bennell, J. D., and Hiddink, J. G. (2018). "Estimating effective detection area of static passive acoustic data loggers from playback experiments with cetacean vocalisations," *Methods Ecol. Evol.* **9**(12), 2362–2371.
- Nuutila, H. K., Thomas, L., Hiddink, J. G., Meier, R., Turner, J. R., Bennell, J. D., Tregenza, N. J. C., and Evans, P. G. H. (2013). "Acoustic detection probability of bottlenose dolphins, *Tursiops truncatus*, with static acoustic dataloggers in Cardigan Bay, Wales," *J. Acoust. Soc. Am.* **134**(3), 2596–2609.
- Pierpoint, C. (2008). "Harbour porpoise (*Phocoena phocoena*) foraging strategy at a high energy, near-shore site in south-west Wales, UK," *J. Mar. Biol. Assoc. U.K.* **88**(6), 1167–1173.
- Pinheiro, J., Bates, D., DebRoy, S., Sarkar, D., and R Core Team (2021). "nlme: Linear and nonlinear mixed effects models," *R* package version 3.1-153, available at <https://CRAN.R-project.org/package=nlme> (Last viewed January 11, 2021).
- R Core Team (2021). "R: A language and environment for statistical computing" (*R* Foundation for Statistical Computing, Vienna, Austria), available at URL <https://www.R-project.org/> (Last viewed January 11, 2021).
- Rojano-Doñate, L. (2020). *Acoustics and Energetics of Echolocators in a Noisy World* (Aarhus Universitet, Denmark).
- Sarnocinska, J., Tougaard, J., Johnson, M., Madsen, P. T., and Wahlberg, M. (2016). "Comparing the performance of C-PODs and SoundTrap/PAMGUARD in detecting the acoustic activity of harbor porpoises (*Phocoena phocoena*)," *Proc. Mtgs. Acoust.* **27**, 070013.
- Schaffeld, T., Brüger, S., Gallus, A., Dähne, M., Krügel, K., Herrmann, A., Jabbusch, M., Ruf, T., Verfuß, U. K., Benke, H., and Koblitz, J. C. (2016). "Diel and seasonal patterns in acoustic presence and foraging behaviour of free-ranging harbour porpoises," *Mar. Ecol. Prog. Ser.* **547**, 257–272.
- Sørensen, P. M., Wisniewska, D. M., Jensen, F. H., Johnson, M., Teilmann, J., and Madsen, P. T. (2018). "Click communication in wild harbour porpoises (*Phocoena phocoena*)," *Sci. Rep.* **8**(1), 9702.
- Stedt, J., Wahlberg, M., Carlström, J., Nilsson, P. A., Amundin, M., Oskolkov, N., and Carlsson, P. (2023). "Micro-scale spatial preference and temporal cyclicity linked to foraging in harbour porpoises," *Mar. Ecol. Prog. Ser.* **708**, 143–161.
- Torres Ortiz, S., Stedt, J., Midtiby, H. S., Egemose, H. D., and Wahlberg, M. (2021). "Group hunting in harbour porpoises (*Phocoena phocoena*)," *Can. J. Zool.* **99**(6), 511–520.
- Villadsgaard, A., Wahlberg, M., and Tougaard, J. (2007). "Echolocation signals of wild harbour porpoises, *Phocoena phocoena*," *J. Exp. Biol.* **210**(1), 56–64.
- Ward, J. A., Morrissey, R. P., Moretti, D. J., DiMarzio, N., Jarvis, S., Johnson, M. P., Tyack, P. L., and White, C. (2008). "Passive acoustic detection and localization of *Mesoplodon densirostris* (Blainville's beaked whale) vocalizations using distributed bottom-mounted hydrophones in conjunction with a digital tag (DTAG) recording," *Can. Acoust.* **36**(1), 60–66.
- Warren, V. E., Marques, T. A., Harris, D., Thomas, L., Tyack, P. L., Aguilar de Soto, N., Hickmott, L. S., and Johnson, M. P. (2017). "Spatio-temporal variation in click production rates of beaked whales: Implications for passive acoustic density estimation," *J. Acoust. Soc. Am.* **141**(3), 1962–1974.
- Wisniewska, D. M., Johnson, M., Teilmann, J., Rojano-Doñate, L., Shearer, J., Sveegaard, S., Miller, L. A., Siebert, U., and Madsen, P. T. (2016). "Ultra-high foraging rates of harbor porpoises make them vulnerable to anthropogenic disturbance," *Curr. Biol.* **26**(11), 1441–1446.
- Wisniewska, D. M., Johnson, M., Teilmann, J., Rojano-Doñate, L., Shearer, J., Sveegaard, S., Miller, L. A., Siebert, U., and Madsen, P. T. (2018b). "Response to 'Resilience of harbor porpoises to anthropogenic disturbance: Must they really feed continuously?'," *Mar. Mammal Sci.* **34**, 265–270.
- Wisniewska, D. M., Johnson, M., Teilmann, J., Siebert, U., Galatius, A., Dietz, R., and Madsen, P. T. (2018a). "High rates of vessel noise disrupt foraging in wild harbour porpoises (*Phocoena phocoena*)," *Proc. R. Soc. B* **285**(1872), 20172314.
- Wisniewska, D. M., Ratcliffe, J. M., Beedholm, K., Christensen, C. B., Johnson, M., Koblitz, J. C., Wahlberg, M., and Madsen, P. T. (2015). "Range-dependent flexibility in the acoustic field of view of echolocating porpoises (*Phocoena phocoena*)," *eLife* **4**, 1–16.